ENVIRONMENTAL RESEARCH
COMMUNICATIONS

INCLUSIVE PUBLISHING TRUSTED SCIENCE

Part of the ENVIRONMENTAL RESEARCH SERIES

PURPOSE-LED PUBLISHING™

LETTER • OPEN ACCESS

Definition of springtime easterly wind bursts in the Indian Ocean and their roles in triggering positive IOD events

To cite this article: Yao Xiao *et al* 2024 *Environ. Res. Commun.* **6** 031005

Environmental Research Communications

LETTER

Definition of springtime easterly wind bursts in the Indian Ocean and their roles in triggering positive IOD events

Yao Xiao[1,2], **Xiaoxiao Tan**[1,2,3,*] **and Youmin Tang**[2,4,*]

[1] Key Laboratory of Marine Hazards Forecasting, Ministry of Natural Resources, Hohai University, Nanjing, People's Republic of China
[2] College of Oceanography, Hohai University, Nanjing, People's Republic of China
[3] Southern Marine Science and Engineering Guangdong Laboratory (Zhuhai), Zhuhai, People's Republic of China
[4] Environmental Science and Engineering, University of North British Columbia, Prince George, Canada
[*] Authors to whom any correspondence should be addressed.

E-mail: xtan@hhu.edu.cn **and** ytang@unbc.ca

Keywords: Indian Ocean Dipole, tropical air-sea interaction, easterly wind bursts, ocean heat content

OPEN ACCESS

RECEIVED
8 January 2024

REVISED
29 February 2024

ACCEPTED FOR PUBLICATION
12 March 2024

PUBLISHED
20 March 2024

Abstract

Using wind reanalysis dataset, we propose a definition for easterly wind bursts (EWBs) occurring in the Indian Ocean and analyze their effects on positive Indian Ocean Dipole (pIOD) events. It was found that there were eight pIOD events during the period from 1980–2020, all of which were accompanied by EWBs occurrence in spring except 2015. The significant impact of EWBs on pIOD events is through the Bjerkness feedback process, strengthening upwelling in the Eastern Indian Ocean (EIO) and triggering a westward zonal current in the equatorial Indian Ocean, both cooling the EIO and in turn strengthening the easterly wind anomalies. Further analysis reveals that the negative upper ocean heat content (OHC) anomalies in EIO, acting as a trigger of Bjerkness feedback process, also plays a critical role in the development of pIOD. Thus, the simultaneous occurrence of EWBs and negative OHC anomalies in spring is an important precursor to pIOD occurrence, although there are possible other triggers.

1. Introduction

The Indian Ocean Dipole (IOD), identified as the second dominant mode of sea surface temperature (SST) anomalies (SSTA) in the tropical Indian Ocean through empirical orthogonal function analysis (Saji *et al* 1999), is believed to influence climate in the Asian monsoon region and other remote regions (Yamagata *et al* 2004, Cai *et al* 2011, Cai *et al* 2014, Li *et al* 2015). The positive phase is characterized by cold SSTA in the southeastern tropical Indian Ocean and warm SSTA in the west (Saji *et al* 1999, Endo and Tozuka 2016, Zhang *et al* 2020a, 2020b). Anomalous SST gradients drive an anomalous Walker circulation, with subsidence in the east and convection in the west, leading to suppressed rainfall over Indonesia and excess rainfall over East Africa (Annamalai *et al* 2003, Yamagata *et al* 2003 2004). Meanwhile, the IOD can generate atmospheric convergence farther west, leading to catastrophic floods in East Africa (Cai *et al* 2011, Cai *et al* 2014, Deshpande *et al* 2014, Qiu *et al* 2015, Endo and Tozuka 2016).

The IOD is a basin-wide ocean-atmosphere coupled phenomenon, which is initiated by anomalous surface winds. Meanwhile Bjerknes feedback and wind–evaporation–SST feedback play important roles in IOD development (Bjerknes 1969, Lu 2020, Wyrtki 1975, Xie and Philander 1994, Xie 1998). Some scholars have also proposed that the influence of ENSO is also a key factor triggering IOD. El Niño events can produce a lower-level anticyclone over the northwestern Indian Ocean in summer with weakened monsoonal winds over Somalia, thereby warming the northwestern Indian Ocean by reduced evaporation and wind-driven upwelling along the coast of East Africa. The warmed northwestern Indian Ocean SST facilitates subsequent IOD development through the Bjerknes feedback over the Indian Ocean (Kug and Kang 2006, Fan *et al* 2017). On the other hand, El Niño weakens the negative precipitation over the maritime continent during the developing phase of the El

Niño. As this negative precipitation anomaly over the maritime continent acts to induce the equatorial easterly over the IO, which activates the positive IOD event via air–sea interaction (Ham *et al* 2017).

Recent studies have indicated that high-frequency and strong wind anomalies (e.g., easterly wind bursts (EWBs)) that occur over the tropical Indian Ocean can influence the initiation and development of IOD events (Moum *et al* 2014, Zhang *et al* 2021). Moum *et al* (2014) concluded that MJO along the equator can excite anomalous upwelling Kelvin waves which lift the thermocline in the Eastern Indian Ocean (EIO), thereby initiating air-sea interaction in the tropical Indian Ocean. Zhang *et al* (2021) noted that the EWBs that occurred in spring played a crucial role in generating an extreme positive IOD (pIOD) event in 2019 by weakening the westerly monsoon circulation, causing oceanic upwelling Kelvin waves, and reducing sea surface height anomalies and SSTA in the EIO. These atmospheric forcings are an important link between synoptic-scale change and climate change, resulting in asymmetry and unpredictability of the IOD (Kug *et al* 2009, Rao *et al* 2009, Wilson *et al* 2013, Feng and Duan 2018, 2019, Zhang *et al* 2021). Meanwhile, an east–west SSTA gradient can further drive easterly wind anomalies and atmospheric convection anomalies, which in turn lead to westward current and thermocline fluctuation, reinforcing the cooling in the east and warming in the west. (Yamagata *et al* 2004, Krishnan *et al* 2011, Xue *et al* 2020, Xiao *et al* 2022).

However, previous studies of EWBs and their effects on IOD events are not sufficiently comprehensive. The role of EWBs has only been discussed through case studies (Zhang *et al* 2021, Zhao and Yuan 2021), and less attention has been paid to the common role of EWBs in triggering IOD events. Many previous studies have analyzed the spatial and temporal characteristics of westerly wind burst (WWB) events over the tropical Pacific and their effects on ENSO events (Seiki and Takayabu 2007, Lian *et al* 2014, Hu and Fedorov 2019, Puy *et al* 2019, Tan *et al* 2020). Inspired by WWB on El Ni ñ o, we attempt to answer in this work why the easterly wind anomalies can be strengthened to develop pIOD events in some years but cannot in other years? Is there a wind burst, similar to WWB for El Nino, here to trigger the development of easterly wind anomalies for pIOD events? If so, how do we define the EWB?

To identify and analyze EWBs and determine their effects on IOD events, we propose a quantitative definition for EWBs, so that their intensity and impact on IOD events can be measured. We focus on the common role of EWBs in pIOD events and discuss the combined effect of EWBs and upper ocean heat content (OHC) on IOD triggering.

The data used in this study and the definition of EWBs are presented in section 2. In section 3, we evaluate the impact of EWBs on IOD events and the co-effect of EWBs and OHC anomalies. Section 4 provides a summary and discussion.

2. Datasets and methods

Analysis was conducted using datasets of daily 10 m wind from the National Centers for Environmental Prediction-Department of Energy (NCEP-DOE) Atmospheric Model Intercomparison Project (AMIP-II) reanalysis (Kanamitsu *et al* 2002), monthly sea surface temperature from Hadley Centre Sea Ice and Sea Surface Temperature data set (HadISST) (Rayner 2003), horizontal current and 300 m OHC from the European Centre for Medium-Range Weather Forecasts (ECMWF) Ocean Reanalysis System 5 (ORA-S5) datasets (Zuo *et al* 2019), and vertical velocity from the Simple Ocean Data Assimilation (SODA) reanalysis (Carton *et al* 2018). These datasets cover the period 1980–2020, and have spatial resolutions of $1.875^\circ \times 1.875^\circ$, $1^\circ \times 1^\circ$, and $1^\circ \times 1^\circ$ (ORAS5 data interpolates irregular grids to $1^\circ \times 1^\circ$), respectively, with 75 vertical layers for ORA-S5 current fields and 50 vertical layers for SODA vertical currents. All anomalies were identified after removing linear trends and climatological seasonal cycles. The Dipole Mode Index (DMI) used in this study is defined as difference of the SSTA, averaged over 50°E–70°E, 10°S–10°N and 90°E–110°E, 10°S–0° (Saji *et al* 1999). If DMI of three consecutive months is greater than 1.5 the standard deviation (STD) in autumn, the year is considered a pIOD event (the opposite case is considered a negative event).

Similar to the definition of westerly wind bursts in the tropical Pacific (Seiki and Takayabu 2007, Lian *et al* 2014, Lopez 2013, Chen *et al* 2015, Fedorov *et al* 2015), in this study, EWBs were identified if: (1) the absolute values of the easterly wind anomalies averaged over 10S-0° were greater than 1.5 the STD; (2) the wind anomalies satisfying condition (1) spanned at least 10 longitudes; (3) the wind anomalies satisfying conditions (1) and (2) lasted for more than 5 days but less than 20 days (This was done to filter out persistent wind anomalies, counting only high-frequency and strong easterly wind anomalies). EWBs were identified in the equatorial Indian Ocean (10°S–0°, 50°E–110°E). On this basis, to describe the intensity of wind bursts, an EWB index was defined as the integration of the easterly wind anomalies related to EWB events:

$$\text{EWB index} = \int\int u' ds dt \, (u' < -1.5 \text{ STD}) \tag{1}$$

where dt and ds denote the duration and spatial span of the identified EWBs, respectively.

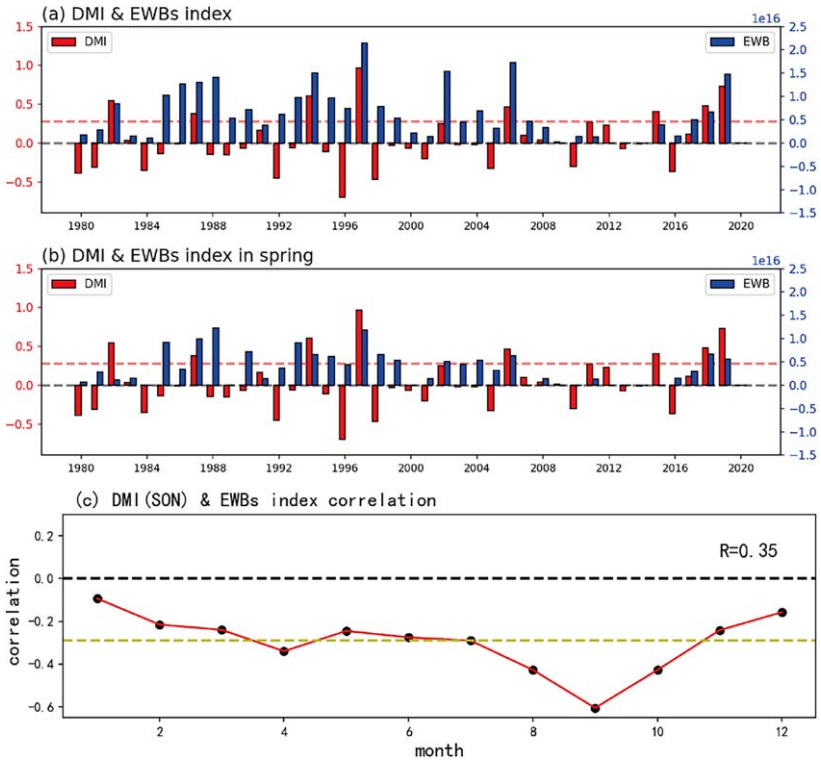

Figure 1. (a) Average DMI in autumn (September-November, red bar, unit: °C) and annual EWB index (blue bar, unit: m^3). The red dashed line represents one standard deviation of the monthly mean DMI; (b) same as (a) but for EWB index in spring; (c) correlation coefficient between DMI in autumn and EWB index with moving window of 3 months. The yellow dotted line represents the 95% confidence test.

The EWBs in the Indian Ocean, like WWBs in the Pacific Ocean, are synoptic-scale change in the atmosphere. However, since the northern Indian Ocean is blocked by Eurasia, the region with the most active air-sea interaction is not equatorial symmetric, so the definition of where EWBs occurs is also asymmetrical. Our definition using the domain between 10°S to the equator is based on partially physical consideration, and partially sensitivity experiments. Both SST anomalies and wind anomalies during IOD initiation and development show equatorial asymmetry with stronger the anomalies in south of the equator (Feng and Meyers 2003, Cai *et al* 2009, Rao *et al* 2009). The results of two senstitvity testings, defining EWBs using the domain of 5°S–5°N and 10°S-10°N, respectively, show the definition by equation (1) is the best in characterizing the relationship between IOD and EWBs, especially for strong IOD events (figure S2, see supplementary).

3. Results

Figure 1(a) depicts the observed evolutions of DMI and equatorial EWB intensity from 1980 to 2020, as expressed by the EWB index. A striking feature is that almost all pIOD events were accompanied by strong EWBs. In particular, an extremely strong pIOD event occurred in 1997, accompanied by EWBs of dramatic intensity (figure 1(a)). EWBs mostly occur in boreal spring and late autumn-winter, corresponding to the onset and mature phase of IOD events (figure S1, see supplementary). To study the relationship between EWBs and IOD events, we calculated the cross-correlation between the DMI in autumn (September-November) and the 3-month running mean of the EWB index; the results are shown in figure 1(c). An obvious feature is that the autumn DMI shows the greatest correlation with the EWB index in October-December, with a correlation coefficient of −0.6. Moreover, although EWBs in spring lead the IOD events by six months, the correlation with the IOD is still statistically significant. The correlation coefficient between EWBs in spring and DMI in autumn was −0.35, passing the 95% confidence test (figure 1(c)). Figure 1(b) shows the relationship between EWBs in spring and IOD in autumn, EWBs in spring are generally stronger in pIOD years. This indicates that spring EWB events may be a precursor of pIOD events, likely triggering them and affecting their development. To explore the role of EWBs in triggering pIOD events, we examined the spring EWBs before the IOD intensity reached its peak. However, EWBs also occur in non-pIOD years (figure 1(a)). The reason for this absence of pIOD events in certain years with strong EWBs is discussed later.

An interesting feature in figure 1(c) is that the correlation drops in summer but rebounds in fall. This is because EWBs rarely occur in summer. The frequent occurrence of EWBs in spring is probably related to monsoon transition in this season. It should be noted that the easterly wind anomalies and EWBs are two different matters in nature although they are highly related. While differing the role of EWBs and the easterly wind anomalies in pIOD events, one may not be surprised why the DMI is not correlated with the EWBs in summer as well as in the spring.

WWBs can excite downwelling kelvin waves and force eastward advection, which subsequently warm the eastern Pacific. In general, strong easterly wind anomalies can cause horizontal water transport at the sea surface, leading to vertical motion through convergence and divergence of surface water (Yamagata *et al* 2004, Moum *et al* 2014, Hu and Fedorov 2019, Zhang *et al* 2021, Zhao and Yuan 2021). Figures 2(a) and (b) show the evolution of EWBs, zonal current anomalies, and vertical current anomalies during the first half of pIOD years. The episodic EWBs generally occur in spring in the central Indian Ocean. These EWBs are accompanied by significant westward flow anomalies, with a maximum magnitude located in the central Indian Ocean, and vertical current anomalies in the EIO, characterized by obvious upwelling off Sumatra-Java, between 90°E and 100°E. These results indicate that EWBs cause a strong wind-driven jet in the equatorial Indian Ocean through shearing, which can transport warm water from the EIO warm-pool region to the Western Indian Ocean (WIO). The conservation of mass requires seawater replenishment, leading to upwelling in the EIO (Cronin and McPhaden 2002; Seiki and Takayabu 2007). With the upwelling of cold water from subsurface ocean, cold SSTA develop in the EIO, contributing significantly to the subsequent cooling of the EIO.

Furthermore, the zonal current anomalies and EIO vertical current anomalies in spring are closely related to the autumn IOD. The correlation between the zonal current anomaly caused by the spring EWBs and the autumn DMI was −0.47, which passed the 95% confidence test (figure 2(c)). The occurrence of upwelling in the EIO during spring is also a feature of pIOD years, showing a statistically significant correlation with the autumn DMI of 0.48 (figure 2(d)). In addition, OHC anomalies intensifies and current anomalies appear almost simultaneously (figure S3, see supplementary). Then the emergence of EWBs strengthens the current anomalies and maintains the OHC anomalies. In summary, EWBs induce the westward equatorial surface current, shallowing the thermocline in the EIO, enhancing the upwelling and decreasing the heat content in EIO, which in turn further strengthen the easterly wind anomalies and westward currents. Through such a Bjerknes positive feedback process, which often lasts a few months, the pIOD can be formed and developed, and finally reaches its peak at the autumn.

Although EWBs tend to produce a dipole-like SSTA in spring, not all such anomalies develop into IOD events (as shown in figures 1(a) and (b)). This raises a new question: under what conditions can EWB events trigger an pIOD? Understanding the reasons for the diversity of IOD responses to EWBs forcing thus remains an important part of predicting IOD. Previous studies suggested that OHC also plays a crucial role in ENSO, which can promote or inhibit the influence of wind forcing (Fedorov *et al* 2015, Levine and McPhaden 2016). Here we examined the two potentially precursors for pIOD events: EWBs and OHC. The OHC anomalies were calculated from ORAS5 reanalysis of the top 300m heat content of the ocean. OHC states were compared under two different conditions: IOD years accompanied by EWBs in spring (pIOD+EWBs, 8 cases) and non-pIOD years with EWBs in spring (NO pIOD + EWBs, 22 cases). A composite of the OHC anomalies is shown in figure 3. In pIOD years (figure 3(a)), there are obvious negative OHC anomalies in the EIO (10°S-5°N, 80°E-110°E) and positive OHC anomalies in the equatorial WIO (5°S-10°N, 40°E-60°E). The distribution of OHC anomalies and strong spring EWBs both favor the occurrence of pIOD through air-sea interaction. Upwelling caused by EWBs transports cold water from deep layers to the surface, and wind stirring intensifies mixing of the upper ocean, both contributing to the cooling in the EIO (Cronin and McPhaden 2002). In the NO pIOD + EWBs years (figure 3(b)), the distribution of OHC anomalies were completely different from that in pIOD years. In NO pIOD years, the EIO featured is neutral OHC anomalies, and a large part of the WIO exhibited negative OHC anomalies, especially in the 10°S-0 range. A strong negative OHC anomalies in the WIO are extremely unfavorable for pIOD development. By comparing figures 3(a) and (b), it can be seen that although EWBs are present, pIOD cannot be triggered when OHC is neutral or even when the EIO warm anomalies are present. In conclusion, although EWBs can cool the EIO to some extent, promoting pIOD development, but are not sufficient on their own. A negative OHC anomaly in the EIO and positive OHC anomaly in the WIO precondition the system for an pIOD event, while EWBs forcing helps to initiate the event; strong EWBs forcing and OHC anomalies are both required for the triggering of an pIOD event.

Figure 4 shows the intensity of EWBs forcing and the OHC anomalies in each spring of the study period, reflecting their combined role in the onset of pIOD events. This reveals that cooling OHC anomalies in the EIO, and EWBs forcing, affect the onset of pIOD events. Furthermore, strong EWBs forcing and OHC anomalies are both critical for extreme IOD events, as observed in 1987,1994,1997, 2006, 2018 and 2019. However, neither EWBs nor OHC cold anomalies occurred in the EIO in the spring of 2015, while in 1982, EWBs occurred in the spring, but the EIO was warm OHC anomalies at this time. The 1982 and 2015 pIOD events do not follow the

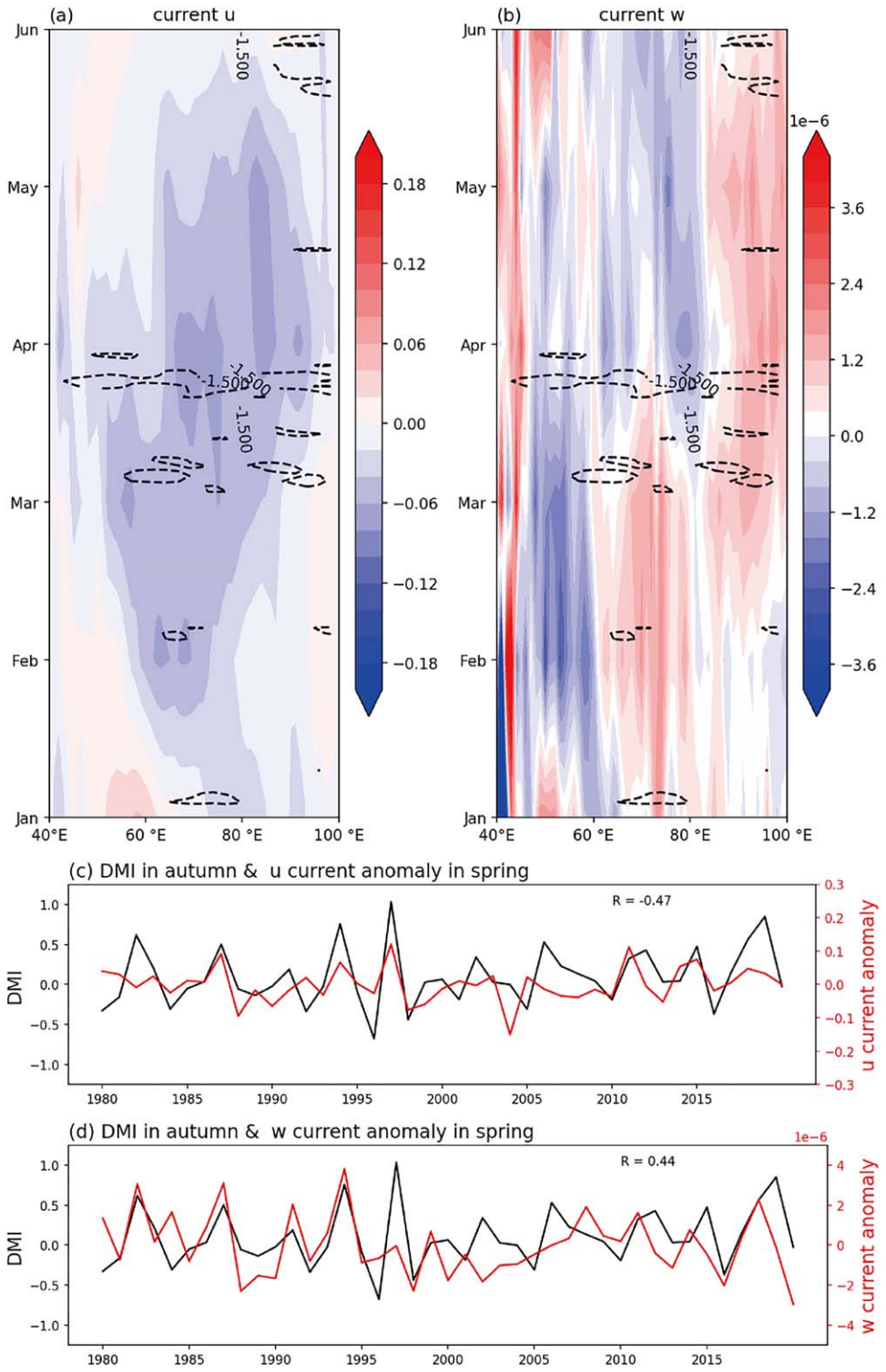

Figure 2. Evolution of EWBs and Equatorial Indian Ocean current anomalies and the correlation between spring current anomalies and DMI. (a)–(b) Composite of the time-longitude evolution of the surface zonal current anomalies (a, color, m/s) and vertical current anomalies in the upper 100 m (b, color, m/s), overlayed with EWBs (contour, unit: m/s) in the tropical Indian Ocean (10°S–0°) in pIOD years. (c)–(d) Time series of DMI in autumn (black, °C) and the zonal current anomaly in spring in the tropical central Indian Ocean (10°S–0°, 70°E-90°E) (c, red, m/s), and the vertical current anomaly in spring in the EIO (10°S–0°, 90°E-100°E) (c, red, m/s)).

pIOD preconditioning of EWBs and OHC anomalies. This is because the warm anomalies in the WIO were significantly stronger than the cold anomalies in the EIO in these two pIOD events. For a normal pIOD event, the cold anomalies in the east are usually stronger than the warm anomalies in the west, resulting in negative OHC anomalies in the EIO. While the warming anomalies are much stronger and dominate the IOD variation, the negative anomalies of OHC could collapse, as seen in these two pIOD events. In general, pIOD events did not

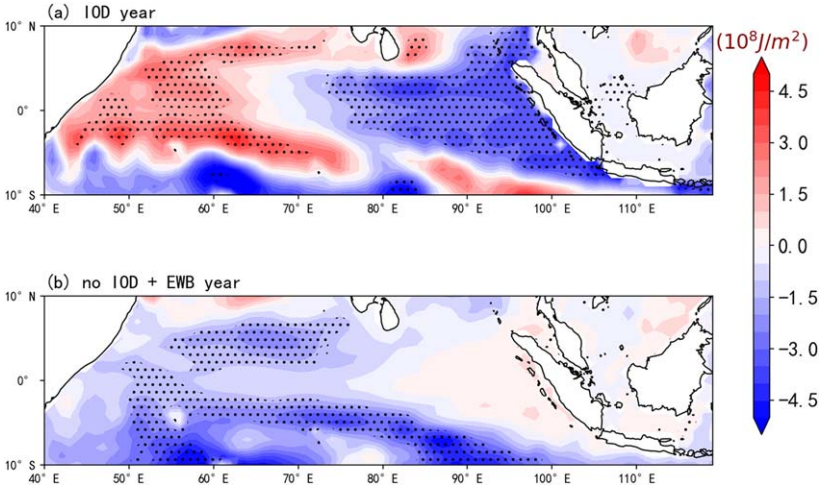

Figure 3. Composite of upper OHC anomalies (unit: $10^8 J/m^2$) in spring (March-May). (a) pIOD + EWBs years; (b) NO pIOD + EWBs years. Hachured regions indicate areas of statistically significant OHC anomalies. Statistical significance is tested by evaluating the difference between the composite mean and climatological mean at the 95% confidence level.

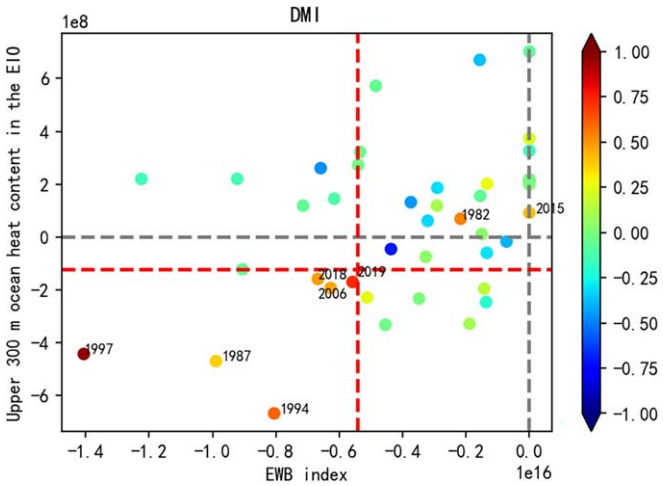

Figure 4. Scatterplot of the upper 300 m OHC anomalies in the EIO (unit: $10^8 J/m^2$) against the EWB index (unit: m^3). The color of the scatterplot indicates the average DMI index in autumn (unit: ℃). The red dotted lines represent the upper tri-sectional quantile of the OHC and EWB index, respectively. The gray dotted lines show the 0 position.

develop when the EWBs were strong, but the EIO exhibited a positive OHC anomaly, or when the EWBs were weak, but the EIO exhibited a negative OHC anomalies. This further indicates that the combined role of EWBs and OHC anomalies are crucial for the occurrence of strong pIOD events.

4. Conclusions

To systematically investigate the high-frequency easterly wind anomalies which occur in the tropical Indian Ocean, and their effects on IOD events, we proposed a definition for EWBs and clarified their role in pIOD events. We found that almost all pIOD events were accompanied by strong EWBs occurring in spring and late autumn except for 2015. The EWBs in spring can significantly affect the vertical current anomalies in the EIO and zonal current anomalies in the central equatorial Indian Ocean. This response of the ocean to strong wind anomalies could be important for the subsequent cooling of the EIO. Thus, EWBs are closely related to the onset of pIOD events.

However, the effects of EWBs are influenced by the initial ocean state. Spring EWB events cannot trigger pIOD events on their own but require the OHC to be negative in spring in the EIO. This phenomenon is more obvious during strong pIOD events. The spring EWBs and negative OHC anomalies in the EIO are necessary conditions for the development of a strong pIOD.

This study determined the combined influence of EWBs and OHC states on pIOD events and provided two potential precursors for IOD occurrence. It should be noted that the results reported are only suggestive, because only a limited number of IOD events were used in the analyses. Meanwhile, correlation analysis and composite method were used in this study, which have limitations in diagnosing causality. This requires to further verify the causality between EWBs, OHC, and IOD, and further refine the physical mechanisms involved.

Acknowledgments

This study was supported by the National Science Foundation Funds of China (42130409, 42176005), National Key Research and Development Program of China (2023YFF0805402), Hohai University (522020512), and the high level personal project of jiangsu province (JSSCRC2021492, JSSCBS 20210256).

Data availability statement

All data that support the findings of this study are included within the article (and any supplementary files).

Open research

The observed and reanalysis datasets were downloaded from the National Centers for Environmental Prediction NCEP-NCAR Reanalysis II (https://psl.noaa.gov/data/gridded/data.ncep.reanalysis2.html), the Hadley Centre Sea Ice and Sea Surface Temperature data set (HadISST) (https://www.metoffice.gov.uk/hadobs/hadisst/data/download.html), the ECMWF ORA-S5 reanalysis datasets (Copernicus Climate Change Service, Climate Data Store, 2021), and the SODA Reanalysis (http://dsrs.atmos.umd.edu/DATA/soda3.15.2/REGRIDED/ocean/).

ORCID iDs

Yao Xiao https://orcid.org/0000-0001-5136-6772

References

Annamalai H, Murtugudde R, Potemra J, Xie S P, Liu P and Wang B 2003 Coupled dynamics over the indian ocean: spring initiation of the zonal mode *Deep-Sea Research Part II: Topical Studies in Oceanography* **50** 2305–30

Bjerknes J 1969 Monthly weather reyiew atmospheric teleconnections from the equatorial pacific *Mon. Weather Rev.* **97** 163–72

Cai W, Pan A, Roemmich D, Cowan T and Guo X 2009 Argo profiles a rare occurrence of three consecutive positive Indian Ocean Dipole events, 2006-2008 *Geophys. Res. Lett.* **36** 2006–8

Cai W, Santoso A, Wang G, Weller E, Wu L, Ashok K, Masumoto Y and Yamagata T 2014 Increased frequency of extreme Indian ocean dipole events due to greenhouse warming *Nature* **510** 254–8

Cai W, Sullivan A, Cowan T, Ribbe J and Shi G 2011 Simulation of the Indian Ocean Dipole: a relevant criterion for selecting models for climate projections *Geophys. Res. Lett.* **38** 1–5

Carton J A, Chepurin G A and Chen L 2018 SODA3: a new ocean climate reanalysis *J. Climate* **31** 6967–83

Chen D, Lian T, Fu C, Cane M A, Tang Y, Murtugudde R, Song X, Wu Q and Zhou L 2015 Strong influence of westerly wind bursts on El Niño diversity *Nat. Geosci.* **8** 339–45

Cronin M F and McPhaden M J 2002 Barrier layer formation during westerly wind bursts *Journal of Geophysical Research: Oceans* **107** 1–12

Deshpande A, Chowdary J S and Gnanaseelan C 2014 Role of thermocline–SST coupling in the evolution of IOD events and their regional impacts *Clim. Dyn.* **43** 163–74

Endo S and Tozuka T 2016 Two flavors of the Indian Ocean dipole *Clim. Dyn.* **46** 3371–85

Fan L, Liu Q, Wang C and Guo F 2017 Indian Ocean dipole modes associated with different types of ENSO development *J. Clim.* **30** 2233–49

Fedorov A V, Hu S, Lengaigne M and Guilyardi E 2015 The impact of westerly wind bursts and ocean initial state on the development, and diversity of El Niño events *Clim. Dyn.* **44** 1381–401

Feng M and Meyers G 2003 Interannual variability in the tropical Indian Ocean: a two-year time-scale of Indian Ocean dipole *Deep-Sea Research Part II: Topical Studies in Oceanography* **50** 2263–84

Feng R and Duan W 2018 The role of initial signals in the tropical Pacific Ocean in predictions of negative Indian Ocean Dipole events *Science China Earth Sciences* **61** 1832–43

Feng R and Duan W 2019 Indian Ocean Dipole-related predictability barriers induced by initial errors in the tropical Indian Ocean in a CGCM *Adv. Atmos. Sci.* **36** 658–68

Ham Y-G, Choi J-Y and Kug J-S 2017 The weakening of the ENSO–Indian Ocean dipole (IOD) coupling strength in recent decades *Clim. Dyn.* **49** 249–61

Hu S and Fedorov A V 2019 The extreme El Niño of 2015–2016: the role of westerly and easterly wind bursts, and preconditioning by the failed 2014 event *Clim. Dyn.* **52** 7339–57

Kanamitsu M, Ebisuzaki W, Woollen J, Yang S K, Hnilo J J, Fiorino M and Potter G L 2002 NCEP-DOE AMIP-II reanalysis (R-2) *Bull. Am. Meteorol. Soc.* **83,** 1631–44

Krishnan R, Sundaram S, Swapna P, Kumar V, Ayantika D C and Mujumdar M 2011 The crucial role of ocean–atmosphere coupling on the Indian monsoon anomalous response during dipole events *Clim. Dyn.* **37** 1–17
Kug J S, Sooraj K P, Jin F F, Luo J J and Kwon M 2009 Impact of Indian Ocean dipole on high-frequency atmospheric variability over the Indian Ocean *Atmos. Res.* **94** 134–9
Kug J-S and Kang I-S 2006 Interactive feedback between ENSO and the Indian Ocean *J. Clim.* **19** 1784–801
Levine A F Z and McPhaden M J 2016 How the July 2014 easterly wind burst gave the 2015–2016 El Niño a head start *Geophys. Res. Lett.* **43** 6503–10
Li G, Xie S P and Du Y 2015 Monsoon-induced biases of climate models over the tropical Indian Ocean *J. Clim.* **28** 3058–72
Lian T, Chen D, Tang Y and Wu Q 2014 Effects of westerly wind bursts on El Niño: a new perspective *Geophys. Res. Lett.* **41** 3522–7
Lopez H and Kirtman B P 2013 Westerly wind bursts and the diversity of ENSO in CCSM3 and CCSM4 *Geophys. Res. Lett.* **40** 4722–7
Lu B and Ren H L 2020 What caused the extreme Indian Ocean dipole event in 2019? *Geophys. Res. Lett.* **47** 0–2
Moum J N *et al* 2014 Air-sea interactions from westerly wind bursts during the november 2011 MJO in the Indian Ocean *Bull. Am. Meteorol. Soc.* **95** 1185–99
Puy M, Vialard J, Lengaigne M, Guilyardi E, DiNezio P N, Voldoire A, Balmaseda M, Madec G, Menkes C and Mcphaden M J 2019 Influence of Westerly Wind Events stochasticity on El Niño amplitude: the case of 2014 vs. 2015 *Clim. Dyn.* **52** 7435–54
Qiu Y, Cai W, Guo X and Ng B 2015 The asymmetric influence of the positive and negative IOD events on China's rainfall *Sci. Rep.* **4** 4943
Rao S A, Luo J-J, Behera S K and Yamagata T 2009 Generation and termination of Indian Ocean dipole events in 2003, 2006 and 2007 *Clim. Dyn.* **33** 751–67
Rayner N A 2003 Global analyses of sea surface temperature, sea ice, and night marine air temperature since the late nineteenth century *J. Geophys. Res.* **108** 4407
Saji N H, Goswami B N, Vinayachandran P N and Yamagata T 1999 A dipole mode in the tropical Indian Ocean *Nature* **401** 360–3
Seiki A and Takayabu Y N 2007 Westerly wind burst and their relationship with intraseasonal variations and ENSO Part I: Statistics *Mon. Weather Rev.* **135** 3325–45
Tan X, Tang Y, Lian T, Yao Z, Li X and Chen D 2020 A study of the effects of westerly wind bursts on ENSO based on CESM *Clim. Dyn.* **54** 885–99
Wilson E A, Gordon A L and Kim D 2013 Observations of the Madden Julian oscillation during Indian Ocean dipole events: IOD-MJO *J. Geophys. Res. Atmos.* **118** 2588–99
Wyrtki K 1975 El Niño—the dynamic response of the equatorial Pacific Oceanto atmospheric forcing *J. Phys. Oceanogr.* **5** 572–84
Xiao Y, Tang Y, Tan X, Wu Y and Yao Z 2022 The SST–wind causal relationship during the development of the IOD in observations and model simulations *Remote Sensing* **14** 1064
Xie S P 1998 Ocean-atmosphere interaction in the making of the walker circulation and equatorial cold tongue *J. Clim.* **11** 189–201
Xie S-P and Philander S G H 1994 . A coupled ocean-atmosphere model of relevance to the ITCZ in the eastern Pacific *Tellus A Dyn Meteorol Oceanogr* **46** 340–50
Xue P, Malanotte-Rizzoli P, Wei J and Eltahir E A B 2020 Coupled Ocean-atmosphere modeling over the maritime continent: a review *JGR Oceans 125* **125** e2019JC014978
Yamagata T, Behera S K, Luo J J, Masson S, Jury M R and Rao S A 2004 Coupled ocean-atmosphere variability in the tropical Indian ocean *Geophysical Monograph Series* **147** 189–211
Yamagata T, Behera S K, Rao S A, Guan Z, Ashok K and Saji H N 2003 Comments on 'Dipoles, temperature gradients, and Tropical Climate Anomalies' [4] *Bull. Am. Meteorol. Soc.* **84** 1418–22
Zhang L, Han W and Hu Z-Z 2021 Interbasin and multiple-time-scale interactions in generating the 2019 extreme Indian Ocean dipole *J. Clim.* **34** 14
Zhang L Y, Du Y, Cai W, Chen Z, Tozuka T and Yu J Y 2020a Triggering the Indian Ocean Dipole from the Southern Hemisphere *Geophys. Res. Lett.* **47** 0–2
Zhang Y, Li J, Zhao S, Zheng F, Feng J, Li Y and Xu Y 2020b Indian Ocean tripole mode and its associated atmospheric and oceanic processes *Clim. Dyn.* **55** 1367–83
Zhao X and Yuan D 2021 Evaluation of intraseasonal wind rectification on recent Indian Ocean dipole events using LICOM *Clim. Dyn.* **58** 981–98
Zuo H, Balmaseda M A, Tietsche S, Mogensen K and Mayer M 2019 The ECMWF operational ensemble reanalysis–analysis system for ocean and sea ice: a description of the system and assessment *Ocean Sci.* **15** 779–808